Energy Reports 6 (2020) 1888–1896

Contents lists available at ScienceDirect

Energy Reports

journal homepage: www.elsevier.com/locate/egyr

Research paper

Co-gasification of oil palm biomass in a pilot scale downdraft gasifier

Kelechi E. Anyaoha [a,1], Ruben Sakrabani [a], Kumar Patchigolla [b,*], Abdul M. Mouazen [c]

[a] Cranfield Soil and Agrifood Institute, Cranfield University, MK43 0AL, United Kingdom
[b] Centre for Thermal Energy Systems and Materials, Cranfield University, MK43 0AL, United Kingdom
[c] Department of Environment, Ghent University, Coupure 653, 900, Gent, Belgium

ARTICLE INFO

Article history:
Received 25 March 2020
Received in revised form 10 June 2020
Accepted 9 July 2020
Available online xxxx

Keywords:
Empty fruit bunch
Palm kernel shell
Mesocarp fibre
Co-gasification

ABSTRACT

The present study focused on co-gasification of empty fruit bunch (EFB), mesocarp fibre (MF) and palm kernel shell (PKS) in a 75 kWth pilot scale downdraft gasifier for possible synergic reactions between the biomass. A series of experiments was carried out using equal blend of EFB, MF, and PKS (particle sizes of 14 and 6.7 mm) and equal blend of MF and PKS. Advanced infrared multi-gas analyser, and thermal conductivity gas analyser were employed to measure the produced gases. The elemental compositions of the raw biomass, ash and slag generated were determined using Scanning Field Emission Gun Scanning Electron Microscopy with accelerating voltage 20.0 kV and working distance 6 mm and the measurements processed using AztecEnergy V2.2 software. The co-gasification of blend of EFB, MF, and PKS, compared to the blend of MF and PKS led to higher gas yield (4.82 and 3.47 m^3/kg_biomass), cold gas efficiency (16.2 and 13.37%), and carbon conversion efficiency (56.3 and 34.18%), respectively. When compared to particle size of 14 mm, the PKS of particle size of 6.7 mm in the EFB/MF/PKS blend increased the lower heating value and the higher heating value of the producer gas by 20% and 20.3%, respectively, and the residue yield was 18.6% less. The overall result has provided evidence on the importance of co-gasification of biomass especially EFB, MF and PKS, which will result in increased utilization of EFB.

1. Introduction

Ash content is an important property of biomass, which influences decisions in biomass thermal conversion operations. Ash forming elements in biomass include alkali earth metals and alkali metals. Ash contain important soil nutrient for soil properties and crop improvement (Shahbaz et al., 2019). Challenges associated with ash in thermal conversion system are bed agglomeration, slagging on the furnace, fouling of heat transfer systems (Kuprianov et al., 2018; Cotton et al., 2014). These will reduce system efficiency and result in increased operational cost (Kuprianov et al., 2018; Aziz et al., 2016). The utilization of biomass in thermal conversion operation will lead to increase in biomass ash generation. The challenge of ash disposal/utilization requires that measures be put in place before and during the thermal conversion process to reduce the amount of ash that would go to landfills and increase agricultural utilization of the residues (Anyaoha et al., 2018a). Increase in the utilization of biomass for energy generation would require the use of a blend of different biomass particularly biomass from the same sources. Therefore, optimizing the effects of co-gasification on thermal conversion process efficiency, thermal conversion infrastructure, and on ash yield and properties is imperative.

Nigeria's biomass resources is estimated to be about 144 million tonnes/year (Toyese and Jibiril, 2016) of which oil palm (*Elaeis guineensis*) fresh fruit bunch (FFB) solid wastes are important part of it. The FFB solid wastes include empty fruit bunch (EFB), mesocarp fibre (MF) and palm kernel shell (PKS), which provide energy used for powering boilers in oil palm mills for FFB processing. The mills are known to be independent in power generation from the abundant FFB wastes. There is reliance on PKS and MF especially during peak periods with little or no effort in the use of EFB for energy production. However, there is increasing interest in the utilization of EFB for energy purpose including in Malaysia (Darmawan et al., 2017; Inayat et al., 2020), which is the second largest palm oil producer in the world after Indonesia (Anyaoha et al., 2018b)

Research on gasification has advanced over the years leading to increased utilization of both fossil fuels and biomass, more importantly the utilization of the blend of coal and biomass. As efforts are being made to increase the utilization of EFB, co-gasification offers a better option. For example Moghadam et al. (2014) co-gasified PKS and polyethylene and produced the highest gas yield of 422.40 g syngas/kg feedstock at the temperature

* Corresponding author.
E-mail address: k.patchigolla@cranfield.ac.uk (K. Patchigolla).
[1] Permanent address: Department of Agricultural Engineering Imo State Polytechnic Umuagwo, Nigeria

https://doi.org/10.1016/j.egyr.2020.07.009

of 800 °C, polyethylene/PKS ratio of 1:0.3, and steam/feedstock ratio of 1:1. Moghadam et al. (2014) concluded that the faster degradation of polyethylene led to increased conversion of the feedstock to gaseous products. Thiagarajan et al. (2018) reported the co-gasification of PKS and low grade Indian coal, while Sulaiman et al. (2018) studied the effects of blending ratio and catalyst loading on co-gasification of wood chips and coconut waste. Monir et al. (2018) observed higher H_2 and CO concentrations from co-gasification of EFB with coal compared to EFB gasification in a downdraft reactor. As efforts are made towards reduction in fossil fuel utilization, there is need to increase the share of biomass in any fuel mix. This is always more important considering the challenges of supply availability of a biomass type (Inayat and Sulaiman, 2018). Therefore, more research is needed on co-gasification of two or biomass without any fossil fuel. Other research on co-gasification are on biomass and coal while few reported on co-gasification of two different biomass (Sulaiman et al., 2018; Monir et al., 2018). No studies have been conducted on the co-gasification of FFB solid wastes except with other fuel types. This study is aimed at bridging the research gap in the co-gasification of FFB solid wastes, uniquely presenting results from co-gasification of three different fuels. The specific objectives are (i) to compare the co-gasification performance of MF/PKS blend, and EFB/MF/PKS blend in a downdraft gasifier, (ii) to determine the effects of PKS particle size on the co-gasification of EFB/MF/PKS blend, and (iii) to evaluate the differences between the residues from the co-gasification of MF/PKS blend, and EFB/MF/PKS blend. This is important to increase the utilization of the three fuels from same source, which eliminates the challenge of biomass availability.

2. Material and methods

2.1. Raw material

Air-dried EFB, MF and PKS, used in the gasification experiment were imported from Nigeria (Fig. 1) and kept in the storage room. The PKS was sorted using 14 mm and 6.7 mm sieve while the EFB was first crushed using a locally made hammer mill at Imo State Polytechnic Umuagwo, Nigeria and sorted with 14 mm sieve. Most of the materials in the PKS greater than 14 mm were poorly cracked and whole palm kernel nuts. The particle size of MF from the mill was smaller than EFB and PKS and therefore was used as received. The proximate and ultimate analyses, and the heating values were analysed for these fuels according to British Standards (2011a) and British Standard (2011b,c).

2.2. Experimental set-up

Fig. 2a, b and c are the pictures of the 75 kW_{th} pilot scale downdraft gasifier, inside of the reactor during one of the co-gasification experiment, and the tar-sampling unit, respectively. Fig. 3a is the schematic diagram of the 75 kW_{th} pilot scale downdraft gasifier used in the co-gasification experiment including the tar sampling unit, while Fig. 3b represents the sampling locations. The gasification unit comprises of a hopper with a slide valve through which materials are introduced into the cylindrical refractory vessel of 240 mm internal diameter and 650 mm height measured from the grate. The height of the gasifier measured from the hopper to the cylindrical refractory vessel is 1350 mm. Air supply hose, ignitor, and thermocouples to record temperatures were inserted at different points on the gasifier chamber. The gasifier is divided into the following zones: biomass, heating up, flaming pyrolysis, reduction upper layer, reduction lower layer and ash pot. The air inlets are positioned to supply air to the heating up, flaming pyrolysis, and reduction layers as shown in Fig. 3a. In between the reduction lower layer and the ash pot is a grate. The electrical ignitor was located below the grate and uses generated heat to ignite biomass. The biomass settled on a grate during the gasification process. The ash collection system was made of two pots, one for bottom ash and the other for fly/cyclone ash. The gaseous products passed through the gas cooling system and are collected for further analysis or discharging to the atmosphere. After each run of experiment, the gasifier was allowed to cool and the fly ash and bottom ash were removed. Two gas analysers: advanced infrared multi-gas analyser MGA300 (Siemens Ultramat 2), and thermal conductivity gas analyser (Siemens Calomat 2) were employed to measure the produced gases.

The tar sampling unit was developed under isokinetic conditions using standard protocol-BSI DD CEB/TS 15439:2006 (British Standard, 2007). The tar sampling unit consisted of (1) gasflow section through which the gas enters the gas preconditioning unit, (2) heated probe, nozzles and valves for pressure reduction and gas cooling (gas preconditioning), (3) particle collection unit to separate and collect solids, (4) tar collection unit for moisture and tar condensation using six impinger bottle, and (5) gas volume measurement unit for gas suction, measurement and off-gas handling. Five of the six bottles were filled with Isopropanol for tar absorption while the sixth bottle was left empty. The bottles were arranged into hot bath (temperature between 35 °C and 40 °C) for 1, 2, and 4, and cold bath (temperature between −15 °C and −20 °C) for 3, 5, and 6. Impinger bottles 2, 3, 5, and 6 were fitted with glass frits at the end of the tube.

The samples of tars and particulate matter were trapped in the heated and/or chilled impinge bottles and heated particulate filter, respectively. Thimble filters were used with a diameter of 30 mm and a length of 100 mm with a retention capacity of 99.9% for particles of size 0.3 μm. The sampled gas volume was measured under dry conditions using a gas meter. The collected tar and particulate samples were stored in a sealed, dark bottle and kept at a temperature below 6 °C for further analysis; the results were not presented in this report. Eliminating tar from the gas stream is important to avoid clogging of pipes and valves, and damage to engine components (Dors and Kurzyńska, 2020).

2.3. Experimental procedures

A series of experiment with equal blend by weight of MF and PKS (50:50) denoted as MP, and equal blend by weight of EFB, MF, and PKS (33:33:33) denoted as EMP1 and EMP2 were carried out using the gasifier. EMP1 had PKS of particle size 14 mm while EMP2 had PKS of particle size 6.7 mm. Fig. 1a, b, c, d and e above are EFB, MF, and PKS, EFB/MF/PKS (6.7 mm particle size) blend, and EFB/MF/PKS (14 mm particle size) blend used in the experiment. The gasifier can hold between 10–15 kg of biomass depending on the characteristics of the fuel. The fuels were fed in batches carefully at a feeding rate of 2.8 kg/h and the process was continuously monitored to ensure there was smooth gasification in the process. The "viewpoint" suited above the grate was used to monitor the presence of flame and as a guide to feeding the biomass. The operating parameters are given in Table 1. The air supply valve was left closed initially while the ignitor was switched on. After about five minutes of igniting the fuel, the ignitor was switched off while the air supply was opened. The gasifier temperature was maintained at 800 °C by varying air/nitrogen ratio. This was done by adjusting the airflow rate or by introducing nitrogen into the reactor.

The gasification process occurs in the following sequence from top to bottom: heating up>flaming pyrolysis>reduction upper layer>reduction lower layer. The "heating up" is the layer at which the biomass was introduced and where the mass gradually

Fig. 1. Fresh fruit bunch solid wastes (a) empty fruit bunch, (b) mesocarp fibre, (c) palm kernel shell, (d) blend (33:33:33) of empty fruit bunch, mesocarp fibre, and palm kernel shell of 6.7 mm particle size, and (e) blend (33:33:33) of empty fruit bunch, mesocarp fibre, and palm kernel shell of 14 mm particle size.

Fig. 2. Pictures from the co-gasification facility (a) the 75 kWh downdraft gasifier, (b) inside the reactor during one of the experiments, (c) the tar-sampling set-up.

heats up from bottom to the top. The biomass devolatilization takes place at the "flaming pyrolysis" zone. Gasification occurs at the "reduction layer", which includes upper layer (reduction reaction) and lower layer (ash bed). The syngas and ash are produced at this layer. The ash and syngas passed through the grate and the bottom ash settled in the ash pot beneath the gasifier. The fly ash settled in the cyclone and the syngas passed through to the cooling system for tar and water condensation. Gas sampling units were used to clean the dirty gaseous products before the measurement by the gas analyser. The gases measured were CO, CO_2, CH_4, and H_2 for MP, EMP1 and EMP2 samples. Finally, the gas passed through a flare and to an exhaust.

The advanced infrared multi-gas analyser was used for measuring CO_2, CO and CH_4 for MP, EMP1 and EMP2 using non-dispersive infrared absorption with solid-state detector, and thermal conductivity gas analyser was used for measuring H_2. The compositions of CO_2, CO, CH_4 and H_2 were measured at intervals of 5 s. Pico Technology data logger was used to monitor the temperature profile continuously throughout the gasifier chamber at 5 s interval for the duration of the operations.

Several assumptions were considered in this study and they are:

- The fuels were evenly mixed
- Stoichiometric air/fuel ratio considered

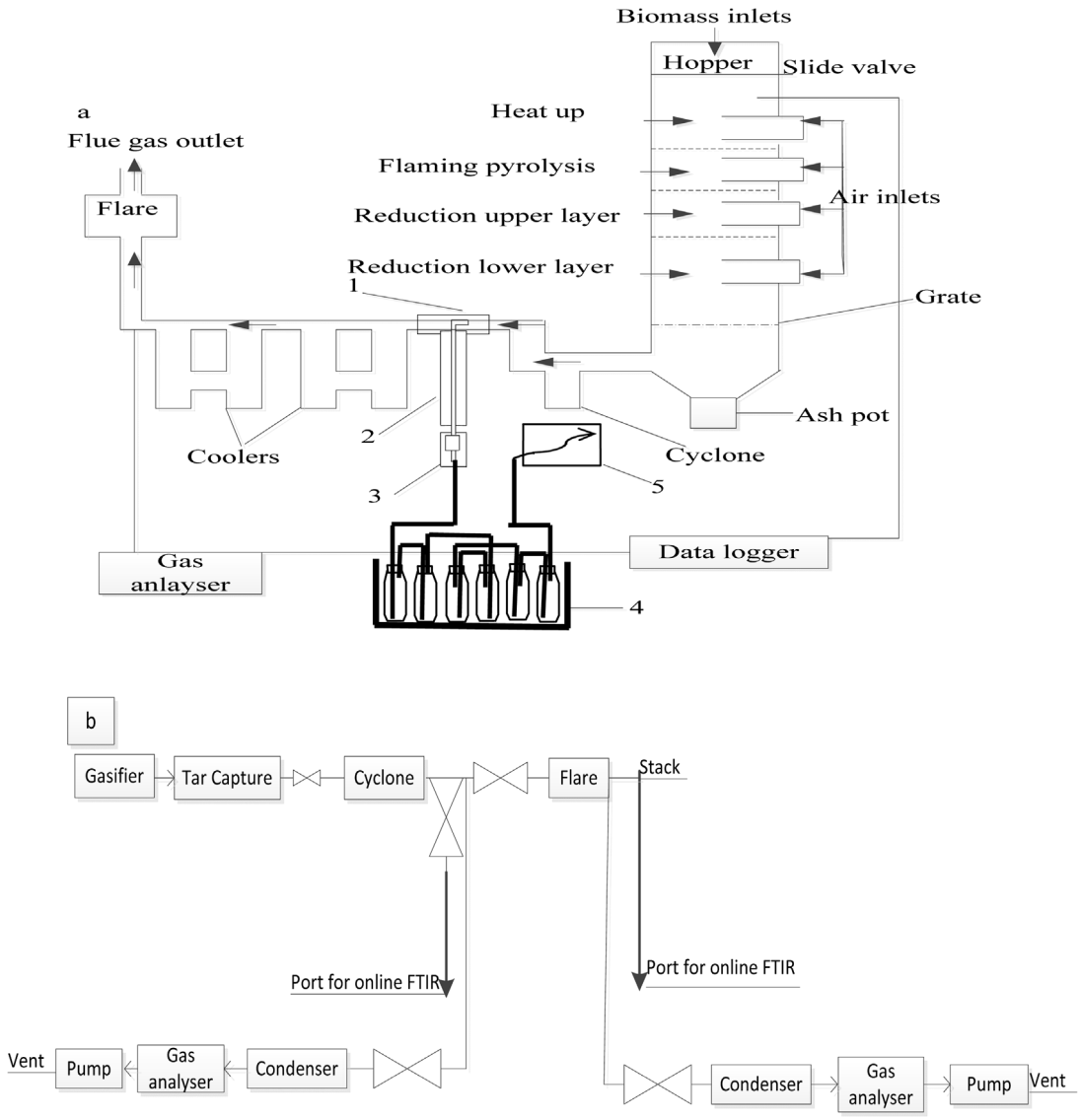

Fig. 3. (a) Schematic diagram of the 75 kW_{th} pilot scale gasifier and tar sampling unit used in co-gasification of empty fruit bunch, mesocarp fibre and palm kernel shell. (b) Gasifier sampling locations during the test. 1 - gas flow section, 2 - gas preconditioning section, 3 - particle collection unit, 4 - tar collection unit, and 5 - gas volume measurement unit.

Table 1
Operating parameters for the fixed-bed downdraft gasifier[a].

Parameter	MP	EMP1	EMP2
Biomass particle size (mm)	14	14	6.7
Temperature (°C)	800	800	800
Biomass feeding rate (kg/h)	2.80	2.80	2.80
Equivalence ratio	0.54	0.59	0.59
Air (l/min)	160	160	160
N_2 (l/min)	<20	<20	<20

[a]MP—mesocarp fibre and palm kernel shell blend, EMP1—palm kernel shell (14 mm), empty fruit bunch and mesocarp fibre blend, EMP2—palm kernel shell (6.7 mm), empty fruit bunch, and mesocarp fibre blend.

- Average biomass calorific value used

The chemical expressions of the biomass used in this study are as shown in Eqs. (1) – (3):

empty fruit bunch $2C_{1.32}H_{2.09}O + 2.685O_2 \rightarrow 2.64CO_2 + 2.09H_2O$ (1)

mesocarp fibre $C_{2.067}H_{3.42}O + 2.422O_2 \rightarrow 2.067CO_2 + 1.71H_2O$ (2)

palm kernel shell $2C_{1.7519}H_{2.33}O + 1.8344O_2 \rightarrow 1.7519CO_2 + 1.165H_2O$ (3)

The equivalence ratio (ER) was calculated according to Eq. (4):

$$ER = \frac{AF_{actual}}{AF_{stoichiometric}} \quad (4)$$

AF_{actual} is the actual air–fuel ratio, which is equal to the amount of fuel injected into the gasifier divided by the amount of biomass. $AF_{stoichiometric}$ is the stoichiometric air–fuel ratio, which is equal to the amount of air needed to burn the biomass divided by the amount of biomass.

The gas yield in $m^3/kg_{biomass}$ was calculated according to Eq. (5) (Kallis et al., 2013):

$$Y_{gas} = \frac{V_{gas}}{Mass_{biomass}} \quad (5)$$

V_{gas} is the volumetric flow-rate of the dry gas in m^3/h calculated using the output gas flow-rate, while $Mass_{biomass}$ is the biomass mass feed rate in kg/h.

The lower heating value of the gas produced (MJ/m^3) was calculated according to Eq. (6) (Kallis et al., 2013), while the higher heating value was estimated according to Eq. (7) (Kallis et al., 2013):

$$LHV_{gas} = \frac{(12.63 * CO + 35.82 * CH_4 + 10.8 * H_2)}{100} \quad (6)$$

$$HHV_{gas} = \frac{(12.63 * CO + 39.82 * CH_4 + 12.75 * H_2)}{100} \quad (7)$$

The values used for CO, CH_4, and H_2 were the compositions of the species in the gas product.

The cold gas efficiency (CGE) and the carbon conversion efficiency (CCE) are important indicators of the gasification process. The cold gas efficiency, which is the ratio of the energy in the produced gas to the energy in the biomass was calculated according to Eq. (8) (Inayat et al., 2016):

$$CGE\% = \left(\frac{Y_{gas} * HHV_{gas}}{HHV_{biomass}}\right) * 100 \quad (8)$$

LHV_{gas} is the lower heating value of the gas product, Y_{gas} is the gas yield in m^3/kg, and $LHV_{biomass}$ is the lower heating value of the biomass used, while HHV_{gas} and $HHV_{biomass}$ are the higher heating values of the gas and biomass, respectively.

The carbon conversion efficiency (CCE), which is the ratio of carbon in the syngas to the carbon in the biomass, was determined according to Eq. (9) (Kallis et al., 2013):

$$CCE\% = \left(\frac{12 * Y_{gas} * (CO\% + CO_2\% + CH_4\%)}{22.4 * C\%}\right) * 100 \quad (9)$$

The compositions of CO, CO_2 and CH_4 in the syngas gas were used in the calculation of the carbon conversion efficiency, and C is the percentage composition of the carbon from the ultimate analysis.

The fly/cyclone ash and bottom ash were collected after each experimental run. The ash was used as soil amendment to test the effects of ash on the properties of a loamy sand soil and cassava yield in Nigeria (results were not part of this paper). The experimental residue yield for each of the experimental test was measured by weighing ash, char and the slag left. The calculated residue yield was according to Eq. (10) (Ogi et al., 2013):

$$Yield\ of\ solid\ residues\ wt.\% = \frac{weight\ of\ solid\ residues}{weight\ of\ biomass\ feedstock} * 100 \quad (10)$$

The elemental compositions of the raw biomass, ash and slag generated were determined using Scanning Field Emission Gun Scanning Electron Microscopy (SFEG SEM) with accelerating voltage of 20.0 kV and working distance of 6 mm. The samples were first coated with Gold and the measurements processed using AztecEnergy V2.2 software.

3. Results and discussion

3.1. Biomass characterization

Table 2 shows the proximate and ultimate analyses of Nigerian EFB, MF and PKS as well as the higher heating value (HHV) and lower heating value (LHV). There is consistency in the HHV and LHV for EFB, MF, and PKS with values decreasing in the following order: MF>PKS>EFB. This is important because MF and PKS are used more than EFB as fuel. The moisture contents as received for the fuels were below 15 % making it suitable for use directly as fuel. The 'dry basis' ash content of EFB and MF are higher than that of PKS by 3.4 and 3.8 units respectively. The fixed carbon and volatile matter contents of the biomass are similar. The results of the HHV of EFB, MF, PKS, blend of MF and PKS, and blend of EFB, MF, and PKS determined by the bomb calorimeter (Parr 6400) are presented in Table 2. The HHVs are close to the values as obtained by the external laboratory.

Table 2
Chemical properties of empty fruit bunch, mesocarp fibre, and palm kernel shell dry basis[a].

Parameter	Empty fruit bunch	Mesocarp fibre	Palm kernel shell
Proximate analyses (%)			
Moisture (as received basis)	14.40	12.10	12.0
Fixed carbon	8.80	8.10	7.60
Ash	5.10	5.50	1.70
Volatile matter	86.10	86.40	90.40
Ultimate analyses (%)			
C	43.80	52.10	52.30
H	5.80	7.20	5.80
N	0.50	1.00	0.40
Cl	0.33	0.38	0.03
S	0.10	0.20	0.02
O (by difference)[b]	44.40	33.6	39.80
HHV (MJ/kg)	18.58 (18.71)	22.17 (22.36)	21.26 (22.33)
LHV (MJ/kg)	17.47	20.84	19.98

HHV—higher heating value, LHV—lower heating value. Values in parenthesis were from the bomb calorimeter, the higher heating values for mesocarp fibre and palm kernel shell blend, and empty fruit bunch, mesocarp fibre and palm kernel shell blend were 21.73 MJ/kg and 19.94 MJ/kg, respectively using the bomb calorimeter.
[a]All in % w/w except where it is stated otherwise.
[b]Oxygen and Total calculations include ash and moisture content.

3.2. Gaseous product yield

The temperature profiles of the experimental runs are presented in Figs. 4–6. The high lignin content of PKS (44%) compared to lignin contents of EFB (21.3%) and MF (27.3%) (Abnisa et al., 2013), the hard structure and bigger particle size contributed to the poor heat transfer and slow start (70 min) to gasification for sample MP (Fig. 4). High lignin content is associated with higher degradation temperature (Sembiring et al., 2015). The initial phase temperatures of EMP1 and EMP2 were within the range of 30 and 40 min (Figs. 5 and 6), which was an indication of the feedstock blend (EFB, MF and PKS). On the other hand, the gasification phase of EMP1, and EMP2 showed similarity and lasted longer than MP. The PKS in MP blend started burning at the later stage of the process but the heat built up overtime was able to complete the process in a shorter time, while the combination of fibrous EFB and MF in EMP1 and EMP2 initiated the process due to their relatively higher quantity than PKS. The fibrous fuels (EFB and MF) burnt faster than PKS, while PKS led to heat build-up gradually resulting in a longer gasification phase. These were evident in the flaming pyrolysis, reduction upper layer, reduction lower layer and heat up temperature profiles for EMP1, and EMP2, which were different from those of MP. The quantity of PKS in MP, which was higher relative to EMP1 and EMP2 also led to overall very low average temperatures for heat up and flaming pyrolysis stages for MP (Fig. 4).

The slow start to rise in temperature for MP delayed the yield of the gaseous species by 75 min (Fig. 7) while EMP1, and EMP2 took less than 15, and 30 min, respectively (Figs. 8 and 9). The variations in biomass of the MP, and EMP1 and EMP2 also led to a more sinusoid-like profile of the gaseous species for EMP1, and EMP2, than MP, which corresponded to the heat build-up inside the reactor. Inayat et al. (2018) obtained similar fluctuations in

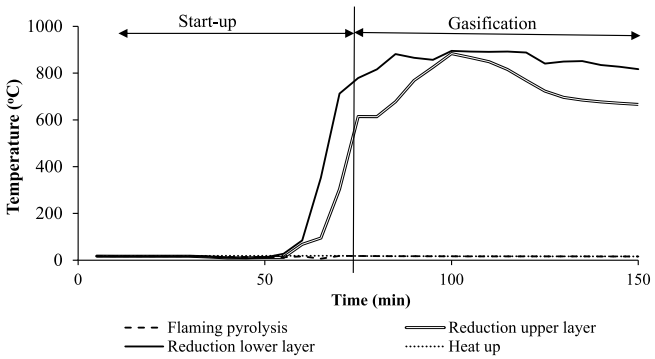

Fig. 4. The temperature profiles from co-gasification of palm kernel shell and mesocarp fibre blend (MP).

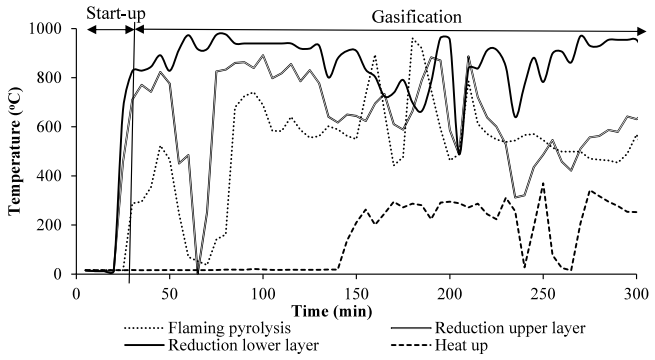

Fig. 5. The temperature profiles from co-gasification of palm kernel shell (14 mm), empty fruit bunch and mesocarp fibre blend (EMP1).

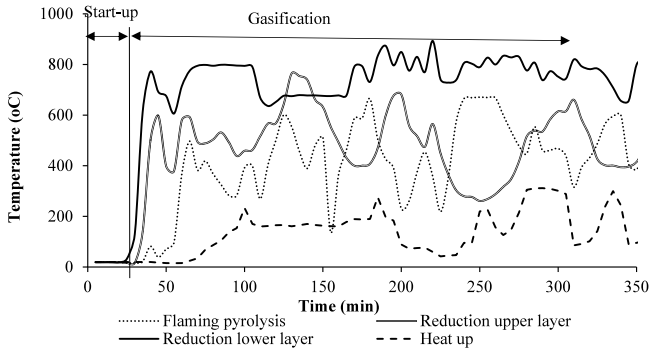

Fig. 6. The temperature profiles from co-gasification of palm kernel shell (6.7 mm), empty fruit bunch and mesocarp fibre blend (EMP2).

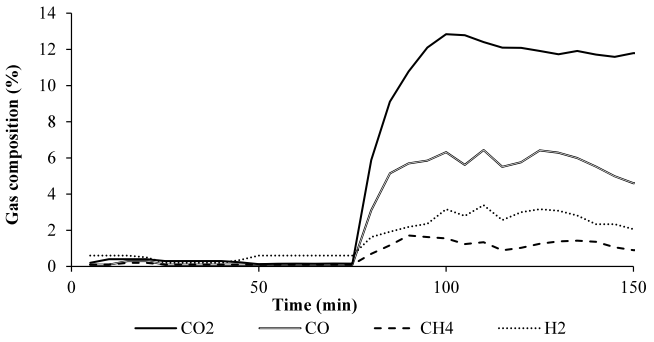

Fig. 7. The gas compositions from co-gasification of palm kernel shell and mesocarp fibre blend (MP).

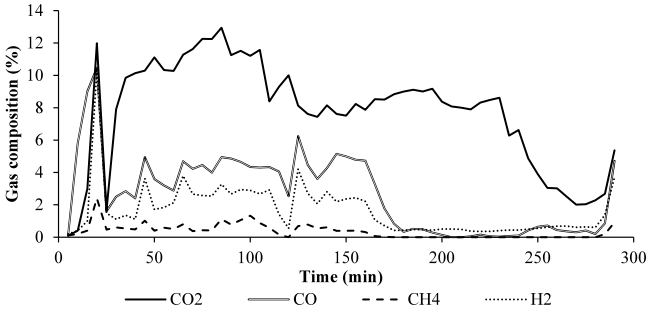

Fig. 8. The gas compositions from co-gasification of palm kernel shell (14 mm), empty fruit bunch and mesocarp fibre blend (EMP1).

gas composition using 10–25 mm particle size. Operating parameters including pressure, temperature, oxygen to biomass ratio, and gasifying agent can influence the fluctuation in syngas yield (Sulaiman et al., 2016). Emami Taba et al. (2012) reported that heterogeneity of biomass or wastes results in increase of fluctuations in quality, availability and composition. This was evident in the composition of the gas as shown in Figs. 7–9. The fluctuation increased with more than two fuels in the co-gasification process as shown in Figs. 7 and 8. Therefore, the optimization of the operating parameters becomes more important with more fuels (Inayat et al., 2019a). Optimizing the equivalence ratio is very important. Most research reported equivalence ratio of 0.1–0.5 (Inayat et al., 2019a,b; Doranehgard et al., 2017; Ariffin et al., 2016). Doranehgard et al. (2017) reported tar content, which increased as ER decreased from 0.5 to 0.1. Inayat et al. (2019a) reported that high ER reduced H_2, tar formation, cold gas efficiency, and gas yield and improved the carbonaceous gas species and carbon conversion efficiency. Ramos et al. (2018) reported an optimum ER of 0.2–0.4 but cautioned that these values depend on other operation conditions. It is worthy to note that the ideal ER can be obtained by controlling the blower speed (Ariffin et al., 2016). The lower heating value of MP gas was higher than those of EMP1, and EMP2 (Table 3), which could be due to the relatively high heating values for the feedstock of MP.

This study recorded lower values of species composition compared to literature. This was due to higher particle sizes of the feedstock used in this study (Mohammed et al., 2011). This led to slow devolatilization and char gasification that are favoured by higher surface area, and therefore poor conversion of the biomass to syngas. The gas yields for MP and EMP1 and EMP2 were lower than Mohammed et al. (2011). The operating conditions and particle size in this study differ from Mohammed et al. (2011). This study used a higher particle size (6.7 mm and 14 mm) against <0.3–1 mm for the Mohammed et al. (2011), which influenced gas yield negatively. However, the homogeneity of the fuel used by Mohammed et al. (2011) must have played a significant role. The gas yield of EMP2 (6.7 mm) was lower than that of EMP1 (14 mm particle size) by 0.2 m^3/kg. Inayat et al. (2016) reported increase in gas yield with particle size of feedstock from biomass co-gasification, which is in line with this study. The CO_2 yield was higher for in all the experiments, which could be attributed to high reactor temperature. Similar results were obtained by Thiagarajan et al. (2018) in PKS and coal co-gasification and Tamili et al. (2018) in co-gasification of grass and coconut.

From Table 3 the LHV_{gas} and HHV_{gas} increased as the particle size decreased. EMP2 with the low particle size of PKS (6.7 mm) in the blend than in EMP1 had lower syngas yield, higher LHV_{gas} and HHV_{gas}. This was because of increased reactivity of the smaller particles leading to better heat transfer (Inayat, 2016). However,

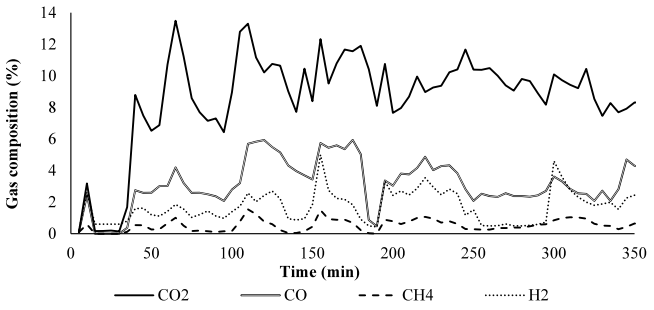

Fig. 9. The gas compositions from co-gasification of palm kernel shell (6.7 mm), empty fruit bunch and mesocarp fibre blend (EMP2).

Table 3
The gasification results for the different biomass blends[a].

Gas composition (mol. %)		MP	EMP1	EMP2
	CO_2	6.01	7.72	8.64
	CO	2.90	2.69	3.18
	CH_4	0.69	0.36	0.53
	H_2	1.54	2.89	1.73
Gas yield (m^3/kgbiomass)		3.47	4.82	4.60
Lower heating $value_{gas}$ (MJ/m^3)		0.78	0.65	0.78
Higher heating $value_{gas}$ (MJ/m^3)		0.84	0.69	0.83
Cold gas efficiency (%)		13.37	16.2	18.54
Carbon conversion efficiency (%)		34.18	56.3	61.65
Yield of solid residues (wt.%)		4.08	4.84	3.94
Yield of ash (wt.%)		1.55	3.16	2.59
Yield of slag (wt.%)		0.39	1.67	1.35
Yield of char (wt.%)		2.14	ns	ns

[a]ns—not significant, MP—mesocarp fibre and palm kernel shell blend, EMP1—palm kernel shell (14 mm), empty fruit bunch and mesocarp fibre blend, EMP2—palm kernel shell (6.7 mm), empty fruit bunch, and mesocarp fibre blend.

LHV_{gas} and HHV_{gas} of EMP2 and MP are approximately the same. This was because the average calorific value of MP feedstock (MS and PKS) was more than that of EMP2 feedstock (EFB, MF and PKS). From Table 2, the calorific values of the blends are average values of the feedstock.

3.3. Residue characteristics

The residues recorded include ash, slag, and char (only PKS char). The residue yield for MP was 2.1% char of the total residue, and more than the sum of ash and slag yields of 1.55 and 0.39%, respectively. This was a result of low carbon conversion as evidenced by the low CCE of 34.18% for MP. Conversely, EMP1 and EMP2 have higher CCE values of 56.3 and 61.65%, and with no char yield, though with higher total residue yield of 4.84 and 3.94%, respectively. The slag yields for EMP1 and EMP2 were higher than that for MP by 1.28 and 0.96%, respectively, which provided evidence of the average potassium content in the feedstock of EMP1, EMP2, and MP, and as shown in the elemental compositions of the raw EFB, MF and PKS, EMP1, EMP2 and MP ash and slag (Tables 4 and 5). EMP2 had lower yield of solid residues (ash and slag), which can be attributed to lower particle size of the PKS used in the feedstock blend (Table 1) resulting in higher reactivity between the fuels. This also led to a higher CCE of 61.65%, higher LHV, HHV and CGE for EMP2 (Table 3) compared to EMP1.

High potassium content EFB ash is a valuable resource in soil amendment, but leads to high agglomeration for example when EFB is used alone. It is important to generate more useable residue from any thermal conversion process especially for agricultural uses. From Tables 4 and 5, the values of alkali and alkali earth metals for the ash and slag are comparably the same and therefore can be used as soil amendment, although slag is undesirable. The sintering behaviour can be explained by the potassium/calcium (K/Ca) ratio. According to Steenari et al. (2009), high silicon, and high K/Ca ratio led to high agglomeration rate in biomass by reducing the ash melting temperature. Tables 4 and 5 show the silicon, potassium, calcium, etc. contents for raw EFB, MF and PKS, the ash and slag of their blends in MP, EMP1 and EMP2. MP recorded lowest K/Ca ratio, which was evident of lower contents of potassium and calcium in the raw MF and PKS feedstock relative to EFB. EMP2 had less K/Ca than EMP1 in line with its low residue yield and more importantly 19% lower slag yield, and as stated above recorded higher carbon conversion efficiency. This was attributed to the lower particle size of PKS in the fuel blend. The lower particle size, less total residue yield, and lower K/Ca ratio, favour lower agglomeration. EFB had lower silicon content, which resulted in lowering the residue yield in the EMP1 and EMP2 blends. The gasification of EFB, MF or PKS will therefore be problematic in terms of agglomeration but the co-gasification from this study increased the chances of synergic reactions considering the differences in elemental compositions of each biomass. Reducing the particle size of the fuel led to more positive effects with EFB in the blend. More importantly the potassium content of the resulting ash increased more than the average values of the constituent fuels. The potassium content of MP ash increased only by 9.2% while the potassium content of EMP1 and EMP2 ash increased by 46.7% and 50%, respectively. This is important from agronomic view for increased agricultural productivity.

Table 4
Elemental compositions of raw empty fruit bunch, mesocarp fibre and palm kernel shell, and MP (mesocarp fibre and palm kernel shell blend) ash as measured using Scanning Field Emission Gun Scanning Electron Microscopy[a].

Parameter	Empty fruit bunch	Mesocarp fibre	Palm kernel shell	MP ash
Na (%)	0.3 ± 0.21	1.72 ± 0.58	1.62 ± 0.66	0.28 ± 0.07
Mg (%)	10.58 ± 1.55	5.01 ± 1.19	9.36 ± 2.74	6.93 ± 0.44
Al (%)	0.47 ± 0.19	4.61 ± 0.66	3.08 ± 0.94	2.4 ± 0.26
Si (%)	25.19 ± 1.69	29.41 ± 4.22	41.36 ± 13.4	42.66 ± 2.69
S (%)	1.39 ± 0.57	5.68 ± 1.19	9.87 ± 1.73	1.78 ± 0.25
Cl (%)	5.65 ± 0.22	12.7 ± 1.04	3.17 ± 0.84	0.92 ± 0.02
K (%)	42.17 ± 1	26.45 ± 1.96	18.6 ± 4.69	24.57 ± 1.33
Ca (%)	13.81 ± 1.28	13.29 ± 2.24	9.29 ± 2.32	16.51 ± 0.73
Fe (%)	0.45 ± 0.36	1.13 ± 0.74	3.66 ± 0.59	3.97 ± 0.1
K/Ca	3.05 ± 0.78	1.99 ± 0.88	2 ± 2.02	1.49 ± 1.82

[a]K/Ca — potassium/calcium ratio.

4. Conclusions

The results from co-gasification of EFB, MF and PKS showed that the addition of EFB to the blend of MF and PKS led to higher gas yield, cold gas efficiency and carbon conversion efficiency, compared to the blend of only MF and PKS. Smaller particle size of PKS increased the lower and higher heating values of the gaseous products, reduced the residue yield and potassium/calcium ratio of EFB/MF/PKS blend. The lower particle size of PKS in the feedstock blend led to relatively lower K/Ca ratio and consequently lower agglomeration. The use of EFB alone will result to high agglomeration due to high potassium content but the addition of MF and PKS will reduce the rate of agglomeration and lead to a valuable residue for use as soil amendment. The co-gasification of EFB, MF and PKS will increase availability of energy sources, reduce the dependency on fossil fuel, and the poor disposal of EFB, which contributes to greenhouse gas emission.

Table 5
Elemental compositions of EMP1 ash [feedstock of blend of palm kernel shell (14 mm), empty fruit bunch and mesocarp fibre], EMP2 ash [palm kernel shell (6.7 mm), empty fruit bunch and mesocarp fibre blend] and MP slag [palm kernel shell and mesocarp fibre blend] and their slag as measured using Scanning Field Emission Gun Scanning Electron Microscopy[a].

Parameter	EMP1 ash	EMP2 ash	MP slag	EMP1 slag	EMP2 slag
Na (%)	0.47 ± 0.18	0.34 ± 0.2	0.58 ± 0.26	0.36 ± 0.1	0.5 ± 0.11
Mg (%)	6.09 ± 0.28	6.57 ± 0.34	4.378 ± 0.46	4.94 ± 1.38	6.77 ± 1.26
Al (%)	1.52 ± 0.14	1.74 ± 0.18	4.42 ± 0.92	13.34 ± 5.63	1.72 ± 0.06
Si (%)	26.71 ± 1.36	24.27 ± 1.19	51.5 ± 4.84	39.01 ± 2.81	41.64 ± 4.66
S (%)	1.88 ± 0.1	1.67 ± 0.16	0.00 ± 0.00	0.1 ± 0.1	0.00 ± 0.00
Cl (%)	6.44 ± 0.45	7.2 ± 0.14	12.7 ± 1.04	1.56 ± 1.39	0.19 ± 0.11
K (%)	42.66 ± 0.78	43.6 ± 0.42	26.45 ± 1.96	26.02 ± 2.09	32.04 ± 1.47
Ca (%)	11.57 ± 0.39	12.02 ± 0.34	13.29 ± 2.24	11.62 ± 3.1	14.62 ± 2.72
Fe (%)	2.66 ± 0.32	2.61 ± 0.39	1.13 ± 0.74	3.06 ± 0.38	2.54 ± 0.36
K/Ca	3.69 ± 0.3	3.63 ± 1.24	1.99 ± 0.88	2.24 ± 0.67	2.19 ± 0.54

[a]K/Ca — potassium/calcium ratio.

CRediT authorship contribution statement

Kelechi E. Anyaoha: Conceptualization, Methodology, Writing - original draft. **Ruben Sakrabani:** Data curation, Supervision, Editing. **Kumar Patchigolla:** Visualization, Reviewing, Editing, Investigation, Validation. **Abdul M. Mouazen:** Supervision.

Declaration of competing interest

The authors declare that they have no known competing financial interests or personal relationships that could have appeared to influence the work reported in this paper.

Acknowledgements

This is part of research project supported by Tertiary Education Trust Fund (TETFUND), Nigeria and Imo State Polytechnic Umuagwo, Ohaji Imo State, Nigeria. The APC is funded by Energy and Power theme at Cranfield University.

References

Abnisa, F., Arami-Niya, A., Wan Daud, W.M.A., Sahu, J.N., 2013. Characterization of bio-oil and bio-char from pyrolysis of palm oil wastes. Bioenergy Res. 6, 830–840, Available at: http://dx.doi.org/10.1007/s12155-013-9313-8.

Anyaoha, K.E., Sakrabani, R., Patchigolla, K., Mouazen, A.M., 2018a. Critical evaluation of oil palm fresh fruit bunch solid wastes as soil amendments: Prospects and challenges resources. Conserv. Recycl. 136, 399–409. http://dx.doi.org/10.1016/j.resconrec.2018.04.022.

Anyaoha, K.E., Sakrabani, R., Patchigolla, K., Mouazen, A.M., 2018b. Evaluating oil palm fresh fruit bunch processing in Nigeria. Waste Manag. Res. 00 (0), 1–11. http://dx.doi.org/10.1177/0734242X17751848.

Ariffin, M.A., Wan Mahmood, W.M.F., Mohamed, R., Mohd Nor, M.T., 2016. Performance of oil palm kernel shell gasification using a medium-scale downdraft gasifier. Int. J. Green Energy 13 (5), 513–520. http://dx.doi.org/10.1080/15435075.2014.966266.

Aziz, M., Budianto, D., Oda, T., 2016. Computational fluid dynamic analysis of co-firing of palm kernel shell and coal. Energies 9 (3), 1–15. http://dx.doi.org/10.3390/en9030137.

British Standard, 2007. Biomass Gasification. Tar and Particles in Product Gases. Sampling and Analysis. DD CEN/TS 15439:2006, British Standard Institute, London, UK, (Accessed: 12 March 2015).

British Standard, 2011b. Solid Recovered Fuels Methods for the Determination of Volatile Matter; Ash Content; Carbon (C), Hydrogen (H) and Nitrogen (N) Content; and Sulphur (S), Chlorine (Cl), Fluorine (F) and Bromine (Br) Content. BS EN 15402-03, 07-08, British Standard Institute, London, UK, (Accessed: 12 March 2015).

British Standard, 2011c. Determination of Moisture Content using the Oven Dry Method. Moisture in General Analysis Sample. BS EN 15414-3, British Standard Institute, London, UK, (Accessed: 12 March 2015).

British Standards, 2011a. Determination of calorific value. BS EN 15400:2011, Available at: https://bsol.bsigroup.com/ (Accessed: 12 Mar 2015).

Cotton, A., Finney, K.N., Patchigolla, K., Eatwell-Hall, R.E.A., Oakey, J.E., Swithenbank, J., Sharifi, V., 2014. Quantification of trace element emissions from low-carbon emission energy sources: (I) Ca-looping cycle for post-combustion CO2 capture and (II) fixed bed, air blown down-draft gasifier. Chem. Eng. Sci. 107, 13–29. http://dx.doi.org/10.1016/j.ces.2013.11.035.

Darmawan, A., Budianto, D., Aziz, M., Tokimatsu, K., 2017. Retrofitting existing coal power plants through cofiring with hydrothermally treated empty fruit bunch and a novel integrated system. Appl. Energy 204 (2017), 1138–1147. http://dx.doi.org/10.1016/j.apenergy.2017.03.122.

Doranehgard, H.M., Samadyar, H., Mesbah, M., Haratipour, P., 2017. High-purity hydrogen production with in situ CO 2 capture based on biomass gasification. Fuel 202, 29–35. http://dx.doi.org/10.1016/j.fuel.2017.04.014.

Dors, M., Kurzyńska, D., 2020. Tar removal by nanosecond pulsed dielectric barrier discharge. Appl. Sci. 10 (991), 1–14. http://dx.doi.org/10.3390/app10030991.

Emami Taba, L., Irfan, M.F., Wan Daud, W.A.M., Chakrabarti, M.H., 2012. He effect of temperature on various parameters in coal, biomass and co-gasification: a review. Renew. Sustain. Energy Rev. 16 (8), 5584–5596. http://dx.doi.org/10.1016/j.rser.2012.06.015.

Inayat, A., Inayat, M., Shahbaz, M., Sulaiman, S.A., Raza, M., Yusup, S., 2020. Parametric analysis and optimization for the catalytic air gasification of palm kernel shell using coal bottom ash as catalyst. Renew. Energy 145, 671–681. http://dx.doi.org/10.1016/j.renene.2019.06.104.

Inayat, M., Sulaiman, S.A., 2018. Effect of blending ratio on quality of producer gas from co-gasification of wood and coconut residual. MATEC Web Conf. 225 (November), http://dx.doi.org/10.1051/matecconf/201822505005.

Inayat, M., Sulaiman, S.A., Hung, T.W., Guangul, F.M., Basrawi, F., 2018. Effect of limestone catalyst on co-gasification of coconut fronds and wood chips. MATEC Web Conf. 225, 1–8. http://dx.doi.org/10.1051/matecconf/201822506009.

Inayat, M., Sulaiman, S.A., Kumar, A., Guangul, F.M., 2016. Effect of fuel particle size and blending ratio on syngas production and performance of co-gasification. J. Mech. Eng. Sci. (JMES) 10 (2), 2188–2200.

Inayat, M., Sulaiman, S.A., Kurnia, J.C., Naz, M.Y., 2019a. Catalytic and noncatalytic gasification of wood–coconut shell blend under different operating conditions. Environ. Prog. Sustain. Energy 38 (2), 688–698. http://dx.doi.org/10.1002/ep.13003.

Inayat, M., Sulaiman, S.A., Kurnia, J.C., Shahbaz, M., 2019b. Effect of various blended fuels on syngas quality and performance in catalytic co-gasification: A review. Renew. Sustain. Energy Rev. 105 (2018), 252–267. http://dx.doi.org/10.1016/j.rser.2019.01.059.

Kallis, K.X., Pellegrini Susini, G.A., Oakey, J.E., 2013. A comparison between miscanthus and bioethanol waste pellets and their performance in a downdraft gasifier. Appl. Energy 101, 333–340. http://dx.doi.org/10.1016/j.apenergy.2012.01.037.

Kuprianov, V.I., Ninduangdee, P., Suheri, P., 2018. Co-firing of oil palm residues in a fuel staged fluidized-bed combustor using mixtures of alumina and silica sand as the bed material. Appl. Therm. Eng. 144, 371–382.

Moghadam, R.A., Yusup, S., Uemura, Y., Chin, B.L.F., Lam, H.L., Shoaibi, A.A., 2014. Syngas production from palm kernel shell and polyethylene waste blend in fluidized bed catalytic steam co-gasification process. Energy 75, 40–44. http://dx.doi.org/10.1016/j.energy.2014.04.062.

Mohammed, M.A.A., Salmiaton, A., Wan Azlina, W.A.K.G., Mohammad Amran, M.S., Fakhru'L.-R.azi, A., 2011. Air gasification of empty fruit bunch for hydrogen-rich gas production in a fluidized-bed reactor. Energy Convers. Manage. 52 (2), 1555–1561. http://dx.doi.org/10.1016/j.enconman.2010.10.023.

Monir, M.U., Abd Aziz, A., Kristanti, R.A., Yousuf, A., 2018. Co-gasification of empty fruit bunch in a downdraft reactor: A pilot scale approach. Bioresour. Technol. Rep. 1, 39–49. http://dx.doi.org/10.1016/j.biteb.2018.02.001.

Ogi, T., Nakanishi, M., Fukuda, Y., Matsumoto, K., 2013. Gasification of oil palm residues (empty fruit bunch) in an entrained-flow gasifier. Fuel 104, 28–35. http://dx.doi.org/10.1016/j.fuel.2010.08.028.

Ramos, A., Monteiro, E., Silva, V., Rouboa, A., 2018. Co-gasification and recent developments on waste-to-energy conversion: A review. Renew. Sustain. Energy Rev. 81, 380–398. http://dx.doi.org/10.1016/j.rser.2017.07.025.

Sembiring, K.C., Rinaldi, N., Simanungkalit, S., 2015. Bio-oil from fast pyrolysis of empty fruit bunch at various temperature. In: Conference and Exhibition Indonesia - New, Renewable Energy and Energy Conservation (the 3rd Indo-EBTKE ConEx 2014) Energy Procedia 65. pp. 162–169. http://dx.doi.org/10.1016/j.egypro.2015.01.052.

Shahbaz, M., Taqvi, S.A., Chun, A., Loy, M., Inayat, A., Uddin, F., Bokhari, S., 2019. Artificial neural network approach for the steam gasification of palm oil waste using bottom ash and CaO. Renew. Energy 132, 243–254.

Steenari, B.M., Lundberg, A., Pettersson, H., Wilewska-Bien, M., Andersson, D., 2009. Investigation of ash sintering during combustion of agricultural residues and the effect of additives. Energy Fuels 23, 5655–5662. http://dx.doi.org/10.1021/ef900471u.

Sulaiman, S.A., Inayat, M., Guangul, F.M., Atnaw, S.M., 2016. Effect of blending ratio on temperature profile and syngas composition of woody biomass co-gasification. J. Chem. Inf. Model. 10 (2), 2176–2186. http://dx.doi.org/10.1017/CBO9781107415324.004.

Sulaiman, S.A., Roslan, R., Inayat, M., Yasi Naz, M., 2018. Effect of blending ratio and catalyst loading on co-gasification of wood chips and coconut waste. J. Energy Inst. 91 (5), 779–785. http://dx.doi.org/10.1016/j.joei.2017.05.003.

Tamili, N., Chuan, L.K., Sulaiman, S.A., Moni, M.N.Z., Inayat, M., Lo, M.Y.K., 2018. Effect of grass and coconut shell blending ratio on the performance of syngas. MATEC Web Conf. 225, 1–6. http://dx.doi.org/10.1051/matecconf/201822502001.

Thiagarajan, J., Srividhya, P.K., Balasubramanian, P., 2018. Thermal behavior and pyrolytic kinetics of palm kernel shells and Indian lignite coal at various blending ratios. Bioresour. Technol. Rep. 4 (July), 88–95. http://dx.doi.org/10.1016/j.biteb.2018.09.004.

Toyese, O., Jibiril, B.E.Y., 2016. Design and feasibility study of a 5MW bio-power plant in Nigeria. Int. J. Renew. Energy Res. 6 (4), 1496–1505. http://dx.doi.org/10.1234/ijrer.v6i4.4755.g6953.